

Intraday Power Trading for Imbalance Markets: An Adaptive Risk-Averse Strategy using Mixture Models

Robin Bruneel, Mathijs Schuurmans, Panagiotis Patrinos

Abstract—Efficient markets are characterised by profit-driven participants continuously refining their positions towards the latest insights. Margins for profit generation are generally small, shaping a difficult landscape for automated trading strategies. This paper introduces a novel, fully-automated cross-border intraday (XBID) trading strategy tailored for single-price imbalance energy markets. This strategy relies on a strategically devised mixture model to predict future system imbalance prices, which, upon benchmarking against several state-of-the-art models, outperforms its counterparts across every metric. However, these models were fit to a finite amount of training data typically causing them to perform worse on unseen data when compared to their training set. To address this issue, a coherent risk measure is added to the cost function to take additional uncertainties in the prediction model into account. This paper introduces a methodology to select the tuning parameter of this risk measure adaptively by continuously quantifying the model accuracy on a window of recently observed data. The performance of this strategy is validated with a simulation on the Belgian energy market using real-time market data. The adaptive tuning approach enables the strategy to achieve higher absolute profits with a reduced number of trades.

Index Terms—Balancing markets, Electricity trading, Mixture models, Risk management, Stochastic optimization

I. INTRODUCTION

THE single-price imbalance settlement scheme is a pricing scheme specifically designed to incentivize market participants who actively contribute to balancing the grid and penalize those who fail to do so [1]. In a single-price imbalance market, a single system imbalance price is settled at fixed time intervals depending on the sign of the system imbalance volume (e.g. every 15 minutes in Belgium). Specifically, a negative system imbalance volume denotes a national energy shortage, requiring the activation of upregulation reserves, resulting in an elevated price. Conversely, a positive system imbalance volume signifies an energy surplus, necessitating the activation of downregulation reserves, leading to a diminished price. Because of balancing incentives by *balance-responsible parties*, the system imbalance price continuously alternates between the two regulation prices. An example of this behaviour has been visualized in Fig. 1. By consuming

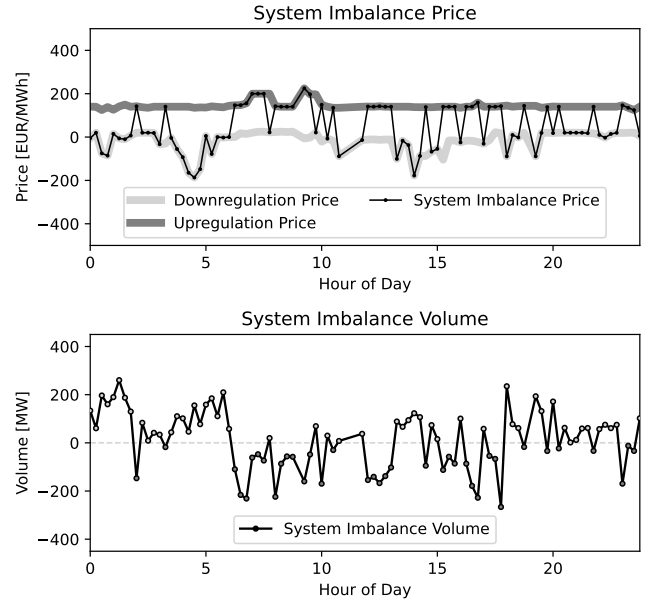


Fig. 1. System imbalance price and volume in Belgium on May 26 2023. Depending on the sign of the system imbalance volume, the system imbalance price continuously alternates between the upregulation and downregulation price. Data obtained from the Belgian transmission system operator ELIA.

additional energy when the imbalance price is low and by producing additional energy when the imbalance price is high, balance-responsible parties not only make profits, but also aid in balancing the national energy grid.

The ability to predict future imbalance prices is a powerful decision making tool in short-term energy markets. On the cross-border intraday energy market, known as XBID, energy is freely traded between balance-responsible parties. By anticipating potential energy shortages or surpluses in the national balancing market, energy may be strategically imported or exported on the cross-border market for profit. This paper delineates an automated trading strategy based on this principle. The strategy comprises two main steps: (i) modelling future system imbalance prices, and (ii) converting these predictions into profitable positions on the intraday energy market. The cross-border intraday energy market closes exactly one hour prior to delivery. Therefore, the designed model needs to provide accurate predictions of the system imbalance price at least one hour ahead.

Manuscript created January, 2024; This work was supported by Flanders Innovation & Entrepreneurship (VLAIO) under grant code "Baekeland Mandaat HBC.2022.0695".

The authors are with the Department of Electrical Engineering (ESAT-STADIUS), KU Leuven, 3001 Leuven, Belgium (email: robin.bruneel@kuleuven.be; mathijs.schuurmans@kuleuven.be; panos.patrinos@kuleuven.be)

A. Related Work

1) *Modelling future system imbalance prices*: The main difficulty in modelling the system imbalance price resides in its inherent alternating behaviour. The prices exhibit a bimodal distribution, which often fails to be captured by traditional predictive models. In the literature, two methodologies to predict system imbalance prices can be distinguished: (i) those that model the balancing state implicitly, and (ii) those that model it explicitly. Implicitly modelling the balancing state involves employing a single model to predict balancing prices, and in doing so, assumes that the typical alternating behaviour is automatically discovered by the model [2]–[4]. Conversely, explicitly modelling the balancing state entails the use of multiple models to predict balancing prices. Typically, one model predicts the probability of arriving in a future balancing state, while separate models compute the prices for each balancing state, thereby reducing the overall model complexity.

A popular approach to explicitly model the balancing state are regime-switching Markov models [5]–[8]. Future balancing states are modelled as a Markov chain, and a distinct price is forecasted for each balancing state. Despite its popularity, a straightforward implementation of regime-switching Markov models in this study reveals two notable issues: (i) static state transition probability matrices are used, independent of other external inputs which might be relevant, and (ii) this method is not suited for longer prediction horizons since the state probabilities converge to a steady-state solution.

Instead of using Markov chains, Koch et al. propose a logistic regression model directly predicting the probability of a future balancing state [9]. This alternative approach mitigates the need to model all intermediate balancing states, rendering it particularly useful for longer prediction horizons. Unlike the static state transition probability matrices, the logistic regression model can easily incorporate other relevant external inputs.

2) *Risk-Averse Trading Strategy*: Given that the distribution of future prices was exactly known, one could simply select a trading strategy that maximizes the expected future return. In practice, however, these distributions are estimated based on models that were fit to a finite amount of training data, and are therefore subject to some amount of error. When applied naively, this typically leads to larger trading losses. A popular approach for taking this model distributional uncertainty – also known as ambiguity – into account, is to replace the expectation by a *coherent risk measure* [10]. Based on the choice of risk measure, larger realizations of the cost will be penalized more, resulting in more risk-sensitive behavior. Furthermore, coherent risk measures can be interpreted as robust counterparts to the expectation. Instead of minimizing the cost over the predicted distribution, the addition of the risk measure can be viewed as a minimization over a specific set of distributions, known as the *ambiguity set* [10, Thm. 6.4]. As a result, this approach robustifies the trading strategy against misestimations of the predicted cost distribution.

Risk-averse optimization is a decision making tool that has been used in power systems before [11]–[14]. Typically, the

tuning parameters are selected in an offline fashion. Bottiau et al. pointed out that using a machine learning model to dynamically adjust the tuning parameters of the risk measure resulted in better performance when applied to very-short-term energy markets [15]. With online learning, the machine learning model is able to adaptively learn the model mismatch.

B. Contribution

In this paper, a fully-automated cross-border energy trading strategy for single-price imbalance markets is proposed. The main focus lies on adaptively quantifying and taking into account the ambiguity in the price prediction model using recent observations. The contributions of this paper are summarized as:

- A novel probabilistic mixture price model for single-price imbalance markets. The performance of this mixture model is benchmarked against several other state-of-the-art models.
- A risk-averse trading strategy to reduce the number of trades in uncertain scenarios. The tuning parameters are optimized in an online fashion based on a window of recently observed data.

The trading strategy is validated with a simulation on the Belgian electricity market using real-time market data.

Notation

Let \mathbb{R} (\mathbb{R}_+) denote the (nonnegative) reals. We denote the n -dimensional probability simplex as $\Delta_n = \{p \in \mathbb{R}_+^n \mid \sum_{i=1}^n p_i = 1\}$. We introduce the shorthand $[n] = \{1, \dots, n\}$ to denote the n smallest positive natural numbers. We denote the positive part of x by $[x]_+ = \max\{x, 0\}$.

II. A MIXTURE IMBALANCE PRICE MODEL

To properly quantify the trading risks and profits, we are interested in predicting the probability density function (pdf) of future system imbalance prices. As mentioned in the introduction, the imbalance price continuously alternates between the regulation prices. Due to this fluctuating behaviour, the future system imbalance price is bimodally distributed. We explicitly take this bimodality into account by modelling the pdf of the imbalance price as a mixture distribution [16]. In this context, the pdf $f : \Xi \rightarrow [0, 1]$ is said to be a mixture of a finite set of component densities $f_i(\cdot; \theta_i)$ with parameters θ_i , $i \in [d]$. A mixture distribution can be written in the form

$$f(\xi) = \sum_{i=1}^d \gamma_i f_i(\xi; \theta_i) \quad (1)$$

where $\gamma \in \Delta_d$ is a vector of nonnegative mixture weights that sum to one. A popular choice for the component densities is the normal distribution $\mathcal{N}(\mu_i, \sigma_i)$ with $\theta_i = (\mu_i, \sigma_i)$. Mixture models are often used when samples are observed from a mixture distribution without knowing from which component distribution they originate. The components are considered *latent variables* and, in that case, specialized algorithms, such as Expectation-Maximization are used to jointly estimate the

component weights γ_i and the parameters θ_i of the distributions, $i \in [d]$. Fortunately, in our application, this difficulty does not arise, as it will be straightforward to infer the active component for each observed data point.

Indeed, in the context of this work, the component densities describe the two regulation price distributions (cf. sec. II-B). The upregulation price, alternatively known as the marginal incremental price (MIP), corresponds to the cost of activating additional reserves. Similarly, the downregulation price, also referred to as the marginal decremental price (MDP), represents the cost associated with reducing production. Depending on the sign of the system imbalance volume, the system imbalance price equals one of the two. In this scenario, the sign of the system imbalance volume is an exogenous variable indicating from which regulation price distribution the imbalance price originates. Thus, the active component density can be directly inferred from the data, negating the need for the formalism of latent variable models.

Using Bayes' theorem, the probability density function of the system imbalance price $f_t^{SI}(p)$ at time t can be expressed as:

$$f_t^{SI}(p) = \pi_t \cdot f_t^{\text{MDP}}(p) + (1 - \pi_t) \cdot f_t^{\text{MIP}}(p) \quad (2)$$

with

$$\begin{aligned} \pi_t &= \mathbb{P}(s_t > 0) \\ f_t^{\text{MDP}}(p) &= f_t^{SI}(p \mid s_t > 0) \\ f_t^{\text{MIP}}(p) &= f_t^{SI}(p \mid s_t \leq 0) \end{aligned} \quad (3)$$

where $s_t \in S_t = \mathbb{R}$ is a random variable representing the future system imbalance volume, and $f_t^{SI}(\cdot \mid E)$ denotes the conditional pdf of the price p_t at time t , given event E . Thus, π_t is the probability to obtain a positive system imbalance volume, f_t^{MDP} is the conditional probability density function of the system imbalance price given a positive system imbalance volume, and f_t^{MIP} the conditional probability density function of the system imbalance price given a negative system imbalance volume. To model future system imbalance price distributions, we may choose to model these components separately to reduce the overall complexity of the problem. A visual representation of this mixture distribution is given in Fig. 2. It is important to note that the mixture weight and distributions are time-dependent (e.g. higher probability on energy shortage and more expensive prices during peak hours), yet, only one system imbalance price p_t is observed at each timestep t . That is, we only observe a single sample from the distribution $f_t^{SI}(p)$, making it practically impossible to estimate the probability density function directly. To address this issue, we assume that the time dependence is introduced through measurable inputs $\mathbf{x}_t \in \mathbb{R}^{n_x}$. With this assumption, we can parametrize the mixture distribution as time-invariant functions with parameters θ_π , θ_{MDP} and θ_{MIP} :

$$\begin{aligned} \pi_t &= \pi(\mathbf{x}_t, \theta_\pi) \\ f_t^{\text{MDP}}(p) &= f^{\text{MDP}}(p; \mathbf{x}_t, \theta_{\text{MDP}}) \\ f_t^{\text{MIP}}(p) &= f^{\text{MIP}}(p; \mathbf{x}_t, \theta_{\text{MIP}}). \end{aligned}$$

These time-invariant models can be estimated with statistical methods. In the upcoming sections, we elaborate on the choice

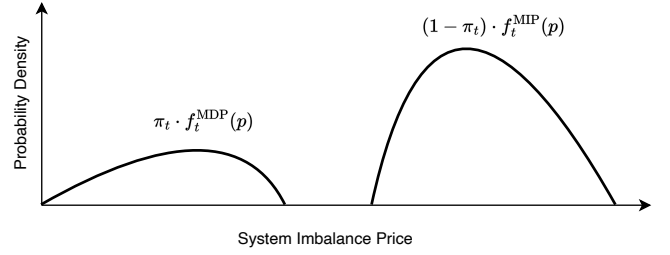


Fig. 2. A sketch of the probability density function of future system imbalance prices. Using a mixture model, we can relieve the model from having to predict this bimodal distribution directly. Instead, we predict the regulation price distributions $f_t^{\text{MDP}}(p)$ and $f_t^{\text{MIP}}(p)$ separately, and combine these using the mixture weight π_t to obtain a prediction of the future system imbalance price distribution.

of these models. The mixture weight is predicted using a logistic regression model, while the regulation price distributions are predicted using multiple quantile regressions.

A. Mixture Weight Model

The mixture weight in Eq. (2), denoted by $\pi_t = \mathbb{P}(s_t > 0)$, represents the probability of a positive system imbalance occurring at timestep t . Various approaches have been proposed for the problem of estimating the probability of such a binary event [17]. Among these approaches is logistic regression, a statistical method used to predict the probability of an event. The simplicity of this model renders it very robust against overfitting at the cost of having linear decision boundaries. Theoretically, this model also requires the log odds of an event to be a linear combination of the input variables [18]. Despite this condition usually not being satisfied, logistic regression still yields meaningful results in practice. Formally, the logistic regression model is a sigmoid layer applied to a linear model:

$$\pi(\mathbf{x}_t, \theta_\pi) = \sigma(\mathbf{w}^\top \mathbf{x}_t + w_0) = \frac{\exp(\mathbf{w}^\top \mathbf{x}_t + w_0)}{1 + \exp(\mathbf{w}^\top \mathbf{x}_t + w_0)} \quad (4)$$

where the weights $\theta_\pi = (w_0, \mathbf{w}) \in \mathbb{R}^{n_x+1}$ are optimized with maximum-likelihood estimation. This model directly outputs the probability that the event occurs.

B. Regulation Price Model

The regulation price models should output the probability density functions of the regulation prices. To predict these density functions, two classes of models can be used: parametric and non-parametric models. Parametric models are trained to output the parameters of a predefined family of distributions (e.g., the mean and variance of a normal distribution). These models are particularly useful if the distribution type is known beforehand. When this is not the case, non-parametric models are typically preferable. These models predict multiple quantiles of an output variable to build a discrete approximation of the cumulative density function (cdf). By differentiating the approximated cdf, the probability density function is obtained. Since (i) there is no obvious choice for a parametric family of distributions that describes the distribution of the regulation price; and (ii) the random variable is scalar, so a fine

discretization of its support is computationally feasible, non-parametric models are used in this paper. Before formulating the parametric form of the price model, we briefly describe the energy reserves, a relevant input signal to determine the regulation price distribution.

1) *Energy reserves*: To compensate for energy shortages or surpluses, transmission system operators (TSOs) activate reserves. For example, in Belgium, two types of reserves (R2 and R3) can be activated. R2 reserves can be activated almost instantly, but are limited in volume. R3 reserves, while slower to activate, are larger in volume. The prices to activate a certain amount of these reserves at time t are known and can be viewed as a mapping o_t from reserve volumes to prices (cf. §II-B2). We propose to predict the regulation prices by internally modelling the activated volumes of each reserve type based on available measurements z_t . Using the aforementioned price mapping, the corresponding price of the reserves can be calculated.

2) *Regulation price model*: For each reserve type $r \in R = \{R2, R3\}$, we discretize the range of reserve volumes $v_r \in V_r = \{v_r^{(1)}, \dots, v_r^{(n_r)}\}$ and use the available data to estimate a discrete probability distribution

$$\mathbf{w}(z_t) = (w_{r,v}(z_t))_{v \in V_r, r \in R} \in \Delta_{n_{R2} + n_{R3}}, \quad (5)$$

as a function of the observed input values z_t . Here, $w_{r,v}(z_t)$ represents the probability that the imbalance price is determined by the price of a given volume $v \in V_r$ of reserve r , given the observation z_t . Using the price mappings $o_{t,r} : V_r \rightarrow \mathbb{R}$, $r \in R$ at time t , we then predict the expected price for the activation of the reserves as

$$g(z_t, \mathbf{o}_t) = \langle \mathbf{w}(z_t), \mathbf{o}_t \rangle, \quad (6)$$

where \mathbf{o}_t is a vector containing the (known) prices for activating a volume of $v \in V_r$ of reserve r at time t :

$$\mathbf{o}_t = (o_{t,r}(v))_{v \in V_r, r \in R} \in \mathbb{R}^{n_{R2} + n_{R3}}$$

The probability vector \mathbf{w}_t in Eq. (5) is modelled using multinomial logistic regression (i.e., a softmax layer). Multinomial logistic regression is an extension of binary logistic regression to predict the probabilities of multiple outcomes [19]. The structure of the proposed regulation price model has been visually depicted in Fig. 3. An intuitive example of how this model works is also given in Table I.

The model proposed in Eq. (6) is used to predict a distribution of regulation prices by applying quantile regression. For each quantile, a model is trained to learn the composition of the reserves for that quantile. For example, more expensive quantiles require a model that gives more weight to expensive reserves. In this context, the choice of an appropriate loss function is crucial. Quantiles of the regulation price can be forecasted by minimizing the *quantile loss* or *pinball loss* [20]. For each quantile $\tau \in [0, 1]$, a different loss L_τ exists, given by:

$$L_\tau(e) = \begin{cases} \tau e & \text{if } e \geq 0 \\ (\tau - 1)e & \text{if } e < 0 \end{cases} \quad (7)$$

By training models for a wide variety of quantiles, a stepwise approximation of the cdf of the regulation price is obtained. In

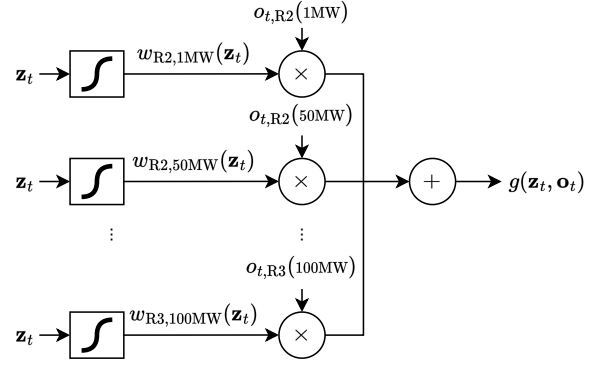


Fig. 3. A visual representation of the price model. Using a multinomial logistic regression model (or softmax layer), the probabilities $\mathbf{w}(z_t)$ that the price equals the price of each reserve activation type are predicted. This probability vector is then multiplied with the order book prices \mathbf{o}_t to obtain a prediction of the regulation price $g(z_t, \mathbf{o}_t)$.

TABLE I
EXAMPLE OF THE UPREGULATION PRICE MODEL

Reserve Type r	Reserve Volume $v_r \in V_r$	$\mathbf{w}(z_t)$	\mathbf{o}_t	$\langle \mathbf{w}(z_t), \mathbf{o}_t \rangle$
R2	1 MW	40%	€120	€154
R2	50 MW	20%	€140	
R2	100 MW	10%	€160	
R3	1 MW	15%	€200	
R3	50 MW	10%	€210	
R3	100 MW	5%	€220	

reality, it is possible that this estimated cumulative distribution is not a monotone increasing function. In that case, quantiles are sorted to satisfy this constraint.

C. Combined Mixture Model

After predicting the mixture weight and regulation price distributions, they are combined using Eq. (2) to obtain a probabilistic forecast of the system imbalance price. If the balancing market were to have more than two possible balancing states, the mixture weight model can be extended to multinomial logistic regression to predict the probability of arriving in each separate balancing state. A similar mixture distribution can then be constructed after predicting the regulation price distribution for each balancing state.

III. TRADING STRATEGY

Energy markets, analogously to stock markets, allow traders to take both long and short positions. A long position involves buying energy on the intraday market and selling it back to the imbalance market. This strategy is profitable if the expected difference between the imbalance price and intraday price is positive. Conversely, a short position involves selling energy in the intraday market and buying it back in the imbalance market, being profitable if the price difference is negative. In this section, we describe a trading strategy that selects long/short positions based on the predicted imbalance price. In practice, prediction models yield lower performance on unseen test sets when compared to their training set. As a

result, naively trusting the model is strongly discouraged. To address this problem, we incorporate a coherent risk measure into the profit function to obtain a risk-aware trading strategy. This risk measure helps to capture the uncertainties inherent in the prediction model, ensuring that the trading strategy remains robust to potential model errors. In this section, we begin by formally defining the risk-averse trading strategy and thereafter, introduce a methodology for optimizing the risk tuning parameters adaptively.

A. Risk-Averse Trading Strategy

The ultimate goal of the trading strategy is to find the trade position on the energy market that maximizes the expected profit, or equivalently, the position that minimizes the expected loss. To ease the notation of the risk measures, we continue with minimization problems. The loss $Z_{p,t}(u)$ for a long strategy with position size $u \in U \subset \mathbb{R}_+$ and delivery time t may be expressed as:

$$Z_{p,t}(u) = (q_t - p)u, \quad p \in P_t$$

where the random variable $p \in P_t$ denotes the future system imbalance price and q_t denotes the (known) intraday price. The optimal position u_t^* that minimizes this expected loss then equals

$$u_t^* = \operatorname{argmin}_{u \in U} \mathbb{E}_p[Z_{p,t}(u)], \quad (8)$$

where the expectation is taken with respect to the random variable p . While q_t is known exactly, the true distribution of the future imbalance price p is not. Using the estimated pdf f_t^{SI} , given in Eq. (2), we may replace the expectation in Eq. (8) by an approximation

$$u_t^* \approx \operatorname{argmin}_{u \in U} \mathbb{E}_{p \sim f_t^{\text{SI}}}[Z_{p,t}(u)]$$

However, using this methodology, the strategy ignores the fact that the price distribution was replaced by a prediction. This may lead to unexpected returns of the strategy when the predicted prices deviate a lot from the true distribution. Instead, we introduce risk-awareness by replacing the expectation with a coherent risk measure ρ_α :

$$u_{\rho_\alpha,t}^* = \operatorname{argmin}_{u \in U} \rho_\alpha[Z_{p,t}(u)] \quad (9)$$

The tuning parameter α controls the level of risk aversion, allowing the trader to balance the desire for higher profits with the need to mitigate risk. An interesting property of coherent risk measures is that they can be viewed as a worst-case expected value over a specific set of distributions, known as the *ambiguity set* [10, Thm. 6.4]. That is, instead of minimizing the expected loss over a single profit distribution f_t^{SI} , we optimize over a set of possible similar distributions \mathcal{A}_t

$$u_{\rho_\alpha,t}^* = \operatorname{argmin}_{u \in U} \max_{f \in \mathcal{A}_t} \mathbb{E}_{p \sim f}[Z_{p,t}(u)]$$

By taking the worst-case realization of the expected loss in the ambiguity set \mathcal{A}_t , the trading strategy is made robust against all realizations within this set. The size of the ambiguity set \mathcal{A}_t varies with the choice of α . A larger ambiguity set leads to a more conservative trading strategy that is less sensitive

to potential model errors, while a smaller ambiguity set leads to a more aggressive trading strategy being more vulnerable to these errors. In this paper, we discuss two commonly used coherent risk measures, namely conditional value at risk and entropic value at risk [21], [22].

The conditional value-at-risk (CVaR), also known as the expected shortfall, equals the expected loss in the worst α cases. CVaR may also be expressed as a convex optimization problem:

$$\text{CVaR}_{1-\alpha}(Z) = \begin{cases} \operatorname{esssup} Z & \text{if } \alpha = 0 \\ \inf_s \left\{ s + \frac{1}{\alpha} \mathbb{E}[Z - s]_+ \right\} & \text{otherwise} \end{cases} \quad (10)$$

where $\alpha \in [0, 1]$. For CVaR, this problem can be solved analytically to obtain the average loss in the worst α cases. By considering only the worst cases, a higher weight is given to the losses making the trading strategy more risk sensitive. This risk measure converges to the expectation (risk-seeking) when $\alpha \rightarrow 1$. Conversely, when $\alpha \rightarrow 0$, this risk measure converges to the maximum value of Z or the largest loss (risk-averse). The entropic value-at-risk (EVaR) is defined as

$$\text{EVaR}_{1-\alpha}(Z) = \begin{cases} \operatorname{esssup} Z & \text{if } \alpha = 0 \\ \inf_{s>0} \left\{ \frac{1}{s} \ln \left(\frac{\mathbb{E}[e^{sZ}]}{\alpha} \right) \right\} & \text{otherwise} \end{cases} \quad (11)$$

Similar to CVaR, EVaR also interpolates between the expectation and the maximum value as α decreases from 1 to 0. An interesting property of coherent risk measures is their positive homogeneity [22], i.e.,

$$\rho_\alpha[aZ] = a \rho_\alpha[Z], \quad \forall a \in \mathbb{R}_+.$$

Using this identity, Eq. (9) can be reformulated as

$$\begin{aligned} u_{\rho_\alpha,t}^* &= \operatorname{argmin}_{u \in U} \rho_\alpha[Z_{p,t}(u)] \\ &= \operatorname{argmin}_{u \in U} \rho_\alpha[(q_t - p)u] \\ &= \operatorname{argmin}_{u \in U} \rho_\alpha[q_t - p]u \\ &= \begin{cases} u_{\max} & \text{if } \rho_\alpha[q_t - p] \leq 0 \\ 0 & \text{if } \rho_\alpha[q_t - p] > 0 \end{cases} \end{aligned} \quad (12)$$

where u_{\max} is the largest value in $U \subset \mathbb{R}_+$. The robust trading strategy will always take either the maximum position or no position at all. We only have to evaluate $\rho_\alpha[q_t - p]$ which can be done efficiently using definitions (10) and (11). A similar derivation can be made to create a robust short strategy.

B. Adaptive Risk Parameters

Risk measures introduce a tradeoff between maximizing potential profits and minimizing associated risks. For CVaR and EVaR, this tradeoff is determined by the tuning parameter α . In very risk-averse scenarios (e.g., safety in autonomous driving [23]), a low, constant α is usually chosen to have high robustness. However, in trading, this would lead to very conservative behaviour where the strategy does not take any positions at all. Instead, we may afford to take larger risks at times when we are more confident about our predictions. To this end, we present a methodology for tuning the risk

parameter α based on a window of previous trades. Concretely, we choose the next α_{t+1} as the value that would have resulted in the smallest absolute loss (in hindsight) over the last N trades:

$$\alpha_{t+1} = \operatorname{argmin}_{\alpha} \frac{1}{N} \sum_{i=0}^{N-1} (q_{t-i} - p_{t-i}) u_{\rho_{\alpha}, t-i}^* \quad (13)$$

where p_t equals the actual system imbalance price at time t , q_t the intraday long price and $u_{\rho_{\alpha}, t}^*$ the risk-averse action that would have been chosen at time t according to Eq. (9) with risk measure ρ_{α} . Using this methodology, the trading strategy will converge to a more risk-averse choice for α when it has consistently generated losses over the past N time steps. Conversely, a more risk-seeking α will be chosen when consistent profits were made.

It is possible to solve problem (13) exactly using the closed-form expression in Eq. (12). Because the value of $u_{\rho_{\alpha}, t}^*$ can only take one of two values (either u_{\max} or 0), the function $\alpha \mapsto u_{\rho_{\alpha}, t}^*$ is piecewise constant. The cost function in Eq. (13), being a linear combination of piecewise constant functions, is therefore also piecewise constant. Thus, to minimize this function, it suffices to enumerate over its N breakpoints.

From this point on, we assume that $\alpha \mapsto \rho_{\alpha}(Z)$ is monotone decreasing for all Z . This is true for both CVaR and EVaR, but also for many other parametric coherent risk measures. Analyzing Eq. (12), under this assumption, we can distinguish the following special edge cases (which are easy to check):

- (i) $\rho_0[q_t - p] \leq 0$. Then, $\rho_{\alpha}[q_t - p] \leq 0$ (and therefore, $u_{\rho_{\alpha}, t}^* = u_{\max}$) for all $\alpha \in [0, 1]$.
- (ii) $\rho_1[q_t - p] > 0$. Then, $\rho_{\alpha}[q_t - p] > 0$ (and therefore, $u_{\rho_{\alpha}, t}^* = 0$) for all $\alpha \in [0, 1]$.

The terms in (13) corresponding to these cases, contribute a constant value of $(q_{t-i} - p_{t-i})u_{\max}$, or 0, respectively, and do not affect the minimizer. Therefore, they can be safely excluded from further consideration.

If neither (i) nor (ii) holds, then $\rho_{\alpha}[q_t - p]$ has a zero-crossing for some $\alpha \in (0, 1]$, which can be computed as¹

$$\alpha_t^b = \min_{\alpha \in (0, 1]} \{\alpha \mid \rho_{\alpha}[q_t - p] \leq 0\}. \quad (14)$$

In that case, we may reformulate Eq. (12) as

$$u_{\rho_{\alpha}, t}^* = H(\alpha - \alpha_t^b) u_{\max}, \quad (15)$$

where $H(x)$ equals the heaviside step function:

$$H(x) = \begin{cases} 1 & \text{if } x \geq 0 \\ 0 & \text{if } x < 0. \end{cases}$$

Thus, substituting (15) into (13), we obtain

$$\alpha_{t+1} = \operatorname{argmin}_{\alpha} \frac{u_{\max}}{N} \sum_{k \in T_t} (q_k - p_k) \cdot H(\alpha - \alpha_k^b), \quad (16)$$

where $T_t \subseteq \{t - N + 1, \dots, t\}$ is the index set containing the time steps where (i) and (ii) do not apply. Problem (16) is solved exactly by evaluating the cost at the breakpoints α_k^b , $k \in T_t$, and selecting α_{t+1} corresponding to the smallest value.

¹This problem is guaranteed to be feasible since $\alpha = 1$ satisfies the constraint due to the exclusion of case (ii).

Algorithm 1: Risk parameter update

Input: Previous set of valid timesteps: T_{t-1} ,
 Previous breakpoints: $(\alpha_k^b)_{k \in T_{t-1}}$,
 Intraday prices: $(q_{t-i})_{i \in \{0, \dots, N-1\}}$,
 Actual imbalance prices: $(p_{t-i})_{i \in \{0, \dots, N-1\}}$
Output: α_{t+1} satisfying eq. (13)

- 1 $T_t \leftarrow T_{t-1} \setminus \{t - N\}$ // Truncate to horizon length
 - 2 **if** $\operatorname{esssup} [q_t - p] > 0$ **and** $\mathbb{E}[q_t - p] \leq 0$ // Not (i) or (ii)
 - 3 **then**
 - 4 $\alpha_t^b \leftarrow \min_{\alpha \in (0, 1]} \{\alpha \mid \rho_{\alpha}[q_t - p] \leq 0\}$ // Solve (14)
(cf. Alg. 2)
 - 5 $T_t \leftarrow T_t \cup \{t\}$
 - 6 Compute permutation $\sigma : T_t \rightarrow T_t$ s.t. $(\alpha_{\sigma(k)}^b)_{k \in T_t}$ is sorted from low to high.
 - 7 $s \leftarrow 0$ // Running sum in (16)
 - 8 $v \leftarrow 0$ // Cost values at the breakpoints α_t^b , $t \in T_t$
 - 9 **for** $k \in T_t$ **do**
 - 10 $s \leftarrow s + (q_{\sigma(k)} - p_{\sigma(k)})u_{\max}$
 - 11 $v_{\sigma(k)} \leftarrow s$
 - 12 $t^* \leftarrow \operatorname{argmin}_{t \in T_t} v_t$
 - 13 $\alpha_{t+1} \leftarrow \alpha_{t^*}^b$
-

In a naive implementation, solving Eq. (13) requires the solution of $|T_t| \leq N$ small-scale problems of the form (14). However, by the receding horizon nature of the problem, T_t can be updated recursively from T_{t-1} by removing $t - N$ and adding t if case (i) and (ii) do not hold. Similarly, the breakpoints α_k^b for $k \in T_{t-1}$ (computed at time $t - 1$) can be stored so that, at worst, only a single breakpoint α_t^b needs to be computed at every subsequent time step t . The overall procedure is summarized in Algorithm 1. Note here that the sorting on line 6 can also be performed incrementally, using the sorted values from the previous time steps.

The most computationally demanding step in Algorithm 1 is solving (14) on line 4. In principle, any scalar root-finding algorithm could be used for this step. However, a more efficient scheme can be obtained by specializing to the risk measures CVaR and EVaR. We discuss both cases individually.

Proposition III.1. For $\rho_{\alpha} = \text{CVaR}_{\alpha}$, (14) is equivalent to

$$\alpha_t^b = \min_{\tau > 0} \mathbb{E}_{p \sim f_t^{\text{SI}}} [\tau(q_t - p) + 1]_+. \quad (17)$$

Proof. Using definition (10), problem (14) may be written as

$$\alpha_t^b = \min_{\alpha \in (0, 1], s} \alpha \quad (18a)$$

$$\text{s.t. } s + \frac{1}{\alpha} \mathbb{E}_{p \sim f_t^{\text{SI}}} [q_t - p - s]_+ \leq 0. \quad (18b)$$

Reordering terms, inequality (18b) is reformulated as:

$$\alpha_t^b = \min_{\alpha \in (0, 1], s} \alpha \quad (19)$$

$$\text{s.t. } \mathbb{E}_{p \sim f_t^{\text{SI}}} [q_t - p - s]_+ \leq -\alpha s,$$

Algorithm 2: Breakpoint α_t^b for CVaR

Input: Predicted distribution: f_t^{SI} ,
 Intraday price: q_t ,
 Predicted quantiles of f_t^{SI} : $(p_{t,i})_{i \in \{1, \dots, n_q\}}$
Output: α_t^b satisfying (17)

```

1 Sort  $(p_{t,i})_{i \in \{1, \dots, n_q\}}$  from low to high
2  $v \leftarrow 0$  // Running sum for the slope
3 for  $i \in \{1, \dots, n_q\}$  do
4    $v \leftarrow v + f_t^{SI}(p_{t,i})(q_t - p_{t,i})$ 
5   if  $v \leq 0$  then
6      $\tau \leftarrow 1/(p_{t,i} - q_t)$ 
7      $B \leftarrow i$ 
8   break
9  $\alpha_t^b \leftarrow \sum_{i=1}^B f_t^{SI}(p_{t,i})(\tau(q_t - p_{t,i}) + 1)$ 

```

The left-hand side of the inequality is always nonnegative and therefore, any feasible value of s (which is guaranteed to exist) is necessarily nonpositive. Moreover, by the exclusion of (i),

$$\rho_0[q_t - p] = \text{esssup } [q_t - p] > 0,$$

and therefore, $\mathbb{E}[q_t - p - s]_+ \stackrel{(s \leq 0)}{\geq} \mathbb{E}[q_t - p]_+ > 0$. (It is a sum of nonnegative terms, of which at least one is strictly positive.) Thus, any feasible s must be strictly negative. Using that $\tau[x]_+ = [\tau x]_+$, for all $x \in \mathbb{R}$ and $\tau \geq 0$, we can divide both sides of the inequality in (19) by $\tau = -s^{-1} > 0$, to obtain (17). \square

Note that in practice, (17) is computed as

$$\alpha_t^b = \min_{\tau > 0} \sum_{i=1}^{n_q} f_t^{SI}(p_{t,i})[\tau(q_t - p_{t,i}) + 1]_+$$

with $p_{t,i}$, $i \in [n_q]$ the quantiles of the forecasted discrete distribution with corresponding densities $f_t^{SI}(p)$. This cost function is piecewise affine, continuous and convex. To find the solution to this problem, we simply calculate the value of τ for which the slope of the piecewise linear segment changes signs. The slope of this scalar function is given by

$$\sum_{i=1}^{n_q} f_t^{SI}(p_{t,i}) \begin{cases} q_t - p_{t,i} & \text{if } p_{t,i} - q_t \leq \frac{1}{\tau} \\ 0 & \text{if } p_{t,i} - q_t > \frac{1}{\tau} \end{cases} \quad (20a)$$

$$= \sum_{i \in J(\tau)} f_t^{SI}(p_{t,i})(q_t - p_{t,i}) \quad (20b)$$

where $J(\tau) = \{i \mid p_{t,i} - q_t \leq \tau^{-1}\}$. Finding the segment where the slope changes signs can be done efficiently by sorting the prices and gradually increasing the size of $J(\tau)$. After plugging the obtained value of τ back in the original equation, we find α_t^b . Algorithm 2 summarizes this procedure.

Proposition III.2. For $\rho_\alpha = \text{EVaR}_\alpha$, (14) is equivalent to

$$\alpha_t^b = \min_{s > 0} \mathbb{E}_{p \sim f_t^{SI}} \left[e^{s(q_t - p)} \right]. \quad (21)$$

Proof. Analogous to CVaR, we substitute the definition of EVaR (11) into (14) to obtain

$$\alpha_t^b = \min_{\alpha \in (0,1], s > 0} \alpha \quad (22a)$$

$$\text{s.t. } \frac{1}{s} \ln \left(\frac{\mathbb{E}_{p \sim f_t^{SI}} [e^{s(q_t - p)}]}{\alpha} \right) \leq 0 \quad (22b)$$

By rearranging some variables, the inequality constraint is rewritten as

$$\alpha_t^b = \min_{\alpha \in (0,1], s > 0} \alpha \quad (23a)$$

$$\text{s.t. } \mathbb{E}_{p \sim f_t^{SI}} \left[e^{s(q_t - p)} \right] \leq \alpha, \quad (23b)$$

which is equivalent to (21). \square

Writing (21) more explicitly in terms of the discretized quantiles $(p_{t,i})_{i \in n_q}$, we obtain

$$\alpha_t^b = \min_{s > 0} \sum_{i=1}^{n_q} f_t^{SI}(p_{t,i}) e^{s(q_t - p_{t,i})}.$$

This is a scalar convex optimization problem which can be rapidly solved to global optimality.

IV. CASE STUDY

In this section, the predictions generated by the previously developed mixture model are used to simulate trading positions on the Belgian electricity market. The strategy is designed to take quarter-hourly positions on the Belgian cross-border intraday energy market (XBID) five minutes before the market closes, which is exactly one hour before delivery. To simulate these positions, real-time order books are used from the Nordpool energy exchange and trades are made with a constant volume of 1 MW. The impact of this trading volume on the imbalance market is expected to be minimal.

A. Statistical Model

To model the Belgian imbalance price, we employ the proposed mixture model. This involves training one mixture weight and two regulation price models. In this case study, the mixture weight model utilizes historical system imbalance volumes and the quarter hour of day (one-hot encoded into 96 binary variables) as input features. The model is trained to output one if the system imbalance price equals the downregulation price and zero if it equals the upregulation price. For the regulation price model, we have to choose the inputs z_t and fixed sets of reserve volumes V_{R2} and V_{R3} . In our experiments, the fixed sets of reserve volumes are

$$V_{R2} = \{1 \text{ MW}, 50 \text{ MW}, 100 \text{ MW}, 150 \text{ MW}, 200 \text{ MW}\}$$

$$V_{R3} = \{1 \text{ MW}, 100 \text{ MW}, 200 \text{ MW}, 300 \text{ MW}, 500 \text{ MW}, 700 \text{ MW}\}$$

We choose the output of the mixture weight model as the input feature $(z_t)_{t \in \mathbb{N}}$ of the regulation price model (cf. §II-B2). This value summarizes the market and is strongly related with the amount of reserves that will be activated. For instance, if the probability of an energy shortage is very large, then

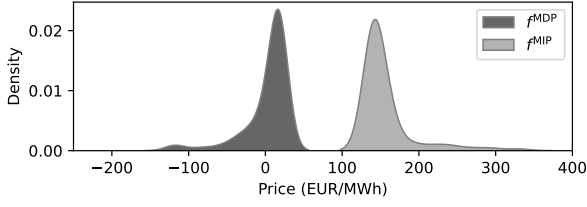


Fig. 4. The predicted distributions f^{MDP} and f^{MIP} on 2023-05-26 18:30 (visualized using kernel density estimation). Both distributions are skewed, they have a low probability to obtain extreme prices when there is a large shortage/surplus of energy.

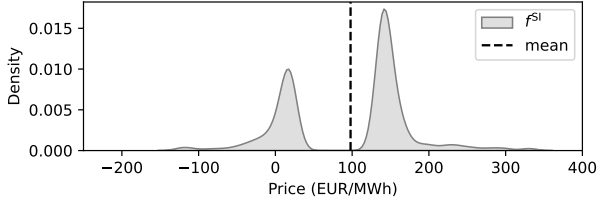


Fig. 5. The predicted system imbalance price distribution f^{SI} on 2023-06-26 18:30 (visualized using kernel density estimation). Because of a high probability on energy shortage, the distribution has higher density for upregulation prices.

there is also a high probability that this shortage will be large. We trained 100 different regulation price models to predict 100 evenly distributed quantiles of the regulation price. The training set spans from June 1, 2021 to April 1, 2023. Testing is performed from April 1, 2023 to October 1, 2023. All the inputs to train this model are obtained from the website of ELIA, the Belgian TSO.

An example of the forecasted regulation price distributions is given in Fig. 4. By weighting the density functions with the mixture weight, a prediction of the system imbalance price distribution is obtained. This has been visualized in Fig. 5.

B. Probabilistic Model Benchmark

To evaluate the performance of the previously proposed price model, it is benchmarked against several *implicit imbalance price models* (cf. §I-A1). These models are designed to predict the system imbalance price directly (without explicitly modeling the bimodality of the distribution) and in doing so, assume that the model implicitly learns to predict the (latent) balancing state. The training set and inputs are the same as in the previous section (previous system imbalance volumes, quarter of the day as one-hot input and the order book prices of the fixed set of reserve volumes \mathbf{o}_t). Each implicit model is trained to output 100 evenly distributed quantiles. Three different probabilistic non-parametric implicit models are presented: (1) linear quantile regression, (2) artificial neural networks (ANN) with one hidden layer, and (3) random forest quantile regression.

- 1) *Linear Model*: The linear quantile regression model is the most simple quantile regression model. The output is a linear combination of the input variables. Quantiles are predicted by minimizing the quantile loss as proposed

TABLE II
LOSSES OF DIFFERENT MODELS ON THE TEST SET. THE MIXTURE MODEL OUTPERFORMS THE OTHER MODELS ON EVERY METRIC

Model	RMSE	Pinball	Std	CRPS
Mixture Model	139.41	83.51	93.73	66.43
Linear	142.61	99.85	116.29	67.85
ANN	142.93	120.04	169.68	71.75
Random Forest	144.59	110.54	135.53	70.40

in Eq. (7). By training separate models for the different quantiles of the system imbalance price, an estimation of its probability density function is obtained.

- 2) *ANN*: Neural network quantile regression models extend traditional linear quantile regression models by replacing the internal model with a neural network. Unlike the linear counterpart, neural network quantile regression can handle complex, nonlinear relationships. To prevent the model from overfitting, one hidden layer with three hidden neurons was chosen. The neurons use the *tanh* activation function.
- 3) *Random Forest*: Random forests are a popular ensemble learning method for regression and classification. By combining a multitude of decision trees, random forests are able to handle nonlinearity and complex interactions between variables. Meinshausen generalized random forests to not only forecast the mean of an output variable, but also forecast conditional quantiles [24]. This generalization is also used in this paper.

Typically, probabilistic forecasts are evaluated on their *reliability* and *sharpness* [25]. Reliable models predict quantiles that are statistically correct with their observations, while the sharpness refers to the concentration of the predictive distributions. More concentrated distributions signify a higher certainty of the model. In this paper, the reliability of the model is assessed by calculating the average pinball loss on the test set. The sharpness is evaluated by calculating the average standard deviation (Std) of the predicted distribution. A lower standard deviation indicates denser prediction intervals. The *continuous ranked probability score (CRPS)* [26] is a widely used metric that assesses both sharpness and reliability of distributions with a single score. It measures the error between the predicted cdf and the true cdf. Consequently, a lower CRPS equals a better probabilistic forecast. We also calculate the root mean square error (RMSE) between the expected value (or mean) of the forecasted distribution and the true observed system imbalance price.

The metrics, calculated on the unseen test set from April 1, 2023 to October 1, 2023, are listed in Table II. The mixture model outperforms the other models on every metric, achieving both a higher sharpness and reliability on the test set. A comparison of the forecasted distributions at one timestep is visualized in Fig. 6. The probabilistic forecasts during a whole day are depicted in Fig. 7.

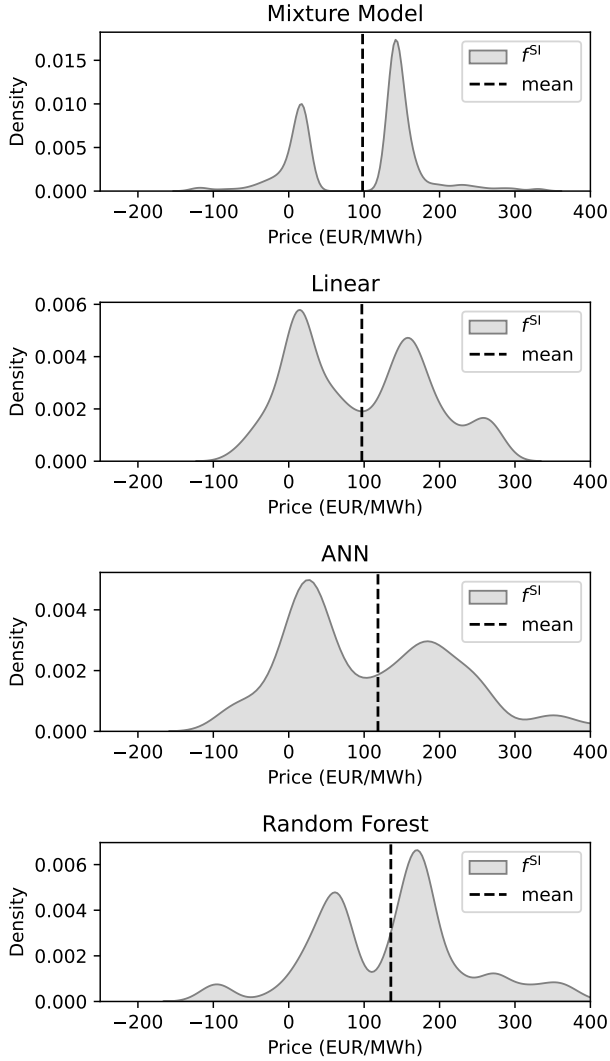


Fig. 6. Predicted system imbalance price probability density function of the different models on 2023-06-26 18:30 (visualized using kernel density estimation). The mixture model has higher densities and makes a better distinction between upregulation and downregulation prices.

C. Risk-Averse Trading Strategy

In this section, the adaptive risk-averse trading strategy is simulated on the Belgian electricity market. In the simulation, a window of 100 previous trades is used to calibrate the tuning parameters. The first month of the test set will be used to calibrate the adaptive trading strategy. After calibrating for a month, the trading strategy is tested from May 2023 to October 2023. This strategy is allowed to take both long and short positions on the energy market and a separate value for α_t is tracked for both position types.

To calculate the optimal α_t , we use the approach as proposed in §III-B. A visualization of the historically simulated profits over a window of recent trades in function of α is shown in Fig. 8. The next α_{t+1} is chosen as the value corresponding to the maximum of this piecewise constant function (this is equivalent to the minimum loss as desired in §III-B). The performances of the different strategies on the test set are visualized in Table III. The adaptive trading strategies clearly

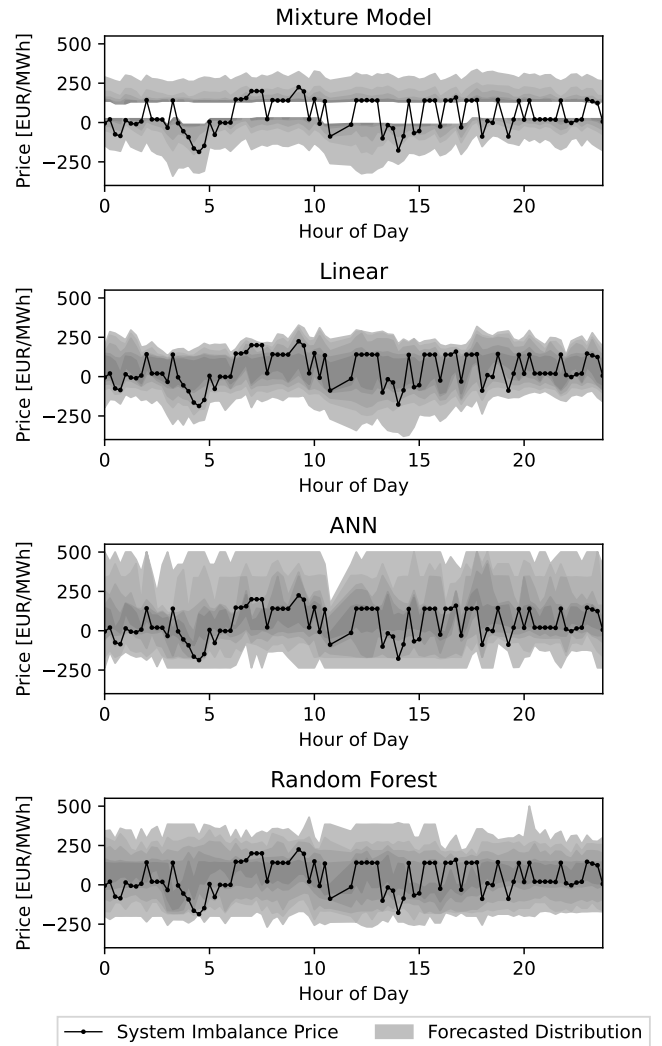


Fig. 7. Forecasted distributions on May 26 2023. The alternating behaviour of the system imbalance price (black line) is clearly visible. Because the mixture model knows that there can be no prices between the lowest upregulation price and highest downregulation price, the probability to obtain such a price is zero. The other models cannot take this constraint into account.

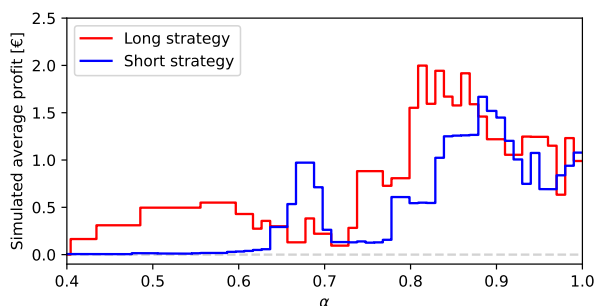
outperform their static counterparts. With only a fraction of the trades, they are able to generate larger profits. Dynamically choosing risk parameters generates the opportunity to trade aggressively when we have high confidence in the model and trade more prudently when the model is not performing so well. After testing the two risk measures, the adaptive trading strategy seems relatively robust against the choice of the risk measure. A histogram of the chosen values for α_t is depicted in Fig. 9. The accumulated profits as visualized in Fig. 10 are consistently increasing.

V. CONCLUSION

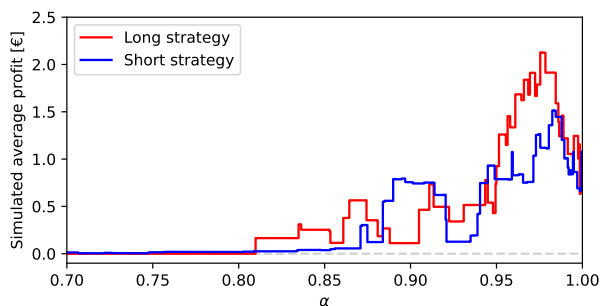
The bimodally distributed system imbalance price is challenging to predict. To address this issue, we employ a novel probabilistic mixture model to predict this price. This reduces the overall complexity of the model and makes it more robust against overfitting. When compared to several state-of-the-art models, the proposed mixture model outperforms its

TABLE III
PERFORMANCE OF THE TRADING STRATEGY ON THE TEST SET USING DIFFERENT RISK MEASURES

Risk Measure	Risk parameter α	Profit [€]	Trades [MW]	Profit Per Trade [€/MW]
Expectation		15384	10404	1.47
CVAR	0.95	16546	8116	2.03
	0.9	13762	6205	2.21
	0.8	12134	3728	3.25
	Adaptive	18561	5570	3.33
EVAR	0.995	15560	8119	1.91
	0.98	13427	6061	2.21
	0.95	13416	3983	3.37
	Adaptive	18559	5414	3.42



(a) CVaR



(b) EVaR

Fig. 8. The historically simulated profits that the trading strategy would have made over the past 100 trading periods for different values of α on 2023-06-26 18:30. For both strategies, the naive approach ($\alpha = 1$) results in suboptimal returns.

counterparts across every metric.

Despite its strong performance, the finite amount of training data makes the model vulnerable to additional prediction errors on unseen data. In efficient markets, even small prediction errors have a large influence on the performance of a trading strategy. By adding a coherent risk measure to the profit function of the trading strategy, distributional uncertainty is taken into account. The parameters of this risk measure are adaptively optimized using a window of recently observed data. After validating this strategy on the Belgian energy market, the adaptive trading strategy results in larger absolute profits with only a fraction of the trades.

REFERENCES

- [1] J. Baetens, J. Laveyne, G. Van Eetvelde, and L. Vandeveld, "Imbalance pricing methodology in Belgium: Implications for industrial consumers," in *2020 17th International Conference on the European Energy Market (EEM)*, 2020, pp. 1–6.
- [2] M. Narajewski, "Probabilistic forecasting of German electricity imbalance prices," *Energies*, vol. 15, p. 4976, 07 2022.
- [3] L. M. Lima, P. Damien, and D. W. Bunn, "Bayesian predictive distributions for imbalance prices with time-varying factor impacts," *IEEE Transactions on Power Systems*, vol. 38, no. 1, pp. 349–357, 2023.
- [4] E. Makri, I. Koskinas, A. C. Tsolakis, D. Ioannidis, and D. Tzovaras, "Short term net imbalance volume forecasting through machine and deep learning: A UK case study," in *Artificial Intelligence Applications and Innovations. AIAI 2021 IFIP WG 12.5 International Workshops*, I. Maglogiannis, J. Macintyre, and L. Iliadis, Eds. Cham: Springer International Publishing, 2021, pp. 377–389.
- [5] D. W. Bunn, J. N. Inekwe, and D. MacGeehan, "Analysis of the fundamental predictability of prices in the British balancing market," *IEEE Transactions on Power Systems*, vol. 36, no. 2, pp. 1309–1316, 2021.
- [6] G. Klæboe, A. L. Eriksrud, and S.-E. Fleten, "Benchmarking time series based forecasting models for electricity balancing market prices," *Energy Systems*, vol. 6, no. 1, pp. 43–61, Mar 2015.
- [7] M. Olsson and L. Soder, "Modeling real-time balancing power market prices using combined SARIMA and Markov processes," *IEEE Transactions on Power Systems*, vol. 23, no. 2, pp. 443–450, 2008.
- [8] J. Dumas, I. Boukas, M. M. de Villena, S. Mathieu, and B. Cornélusse, "Probabilistic forecasting of imbalance prices in the Belgian context," in *2019 16th International Conference on the European Energy Market (EEM)*, 2019, pp. 1–7.
- [9] C. Koch, "Intraday imbalance optimization: incentives and impact of strategic intraday bidding behavior," *Energy Systems*, vol. 13, no. 2, pp. 409–435, May 2022.
- [10] A. Shapiro, D. Dentcheva, and A. Ruszczyński, *Lectures on Stochastic Programming: Modeling and Theory, Third Edition*. Philadelphia, PA: Society for Industrial and Applied Mathematics, 2021.
- [11] K. Bruninx, H. Pandžić, H. Le Cadre, and E. Delarue, "On the interaction between aggregators, electricity markets and residential demand response providers," *IEEE Transactions on Power Systems*, vol. 35, no. 2, pp. 840–853, 2020.
- [12] H. Rashidzadeh-Kermani, M. Vahedipour-Dahraie, M. Shafie-Khah, and P. Siano, "A regret-based stochastic bi-level framework for scheduling of DR aggregator under uncertainties," *IEEE Transactions on Smart Grid*, vol. 11, no. 4, pp. 3171–3184, 2020.
- [13] S. Ghavidel, M. J. Ghadi, A. Azizvahed, J. Aghaei, L. Li, and J. Zhang, "Risk-constrained bidding strategy for a joint operation of wind power and CAES aggregators," *IEEE Transactions on Sustainable Energy*, vol. 11, no. 1, pp. 457–466, 2020.
- [14] J.-F. Toubeau, Z. De Grève, and F. Vallée, "Medium-term multimarket optimization for virtual power plants: A stochastic-based decision environment," *IEEE Transactions on Power Systems*, vol. 33, no. 2, pp. 1399–1410, 2018.
- [15] J. Bottieau, K. Bruninx, A. Sanjab, Z. De Grève, F. Vallée, and J.-F. Toubeau, "Automatic risk adjustment for profit maximization in renewable dominated short-term electricity markets," *International Transactions on Electrical Energy Systems*, vol. 31, 12 2021.

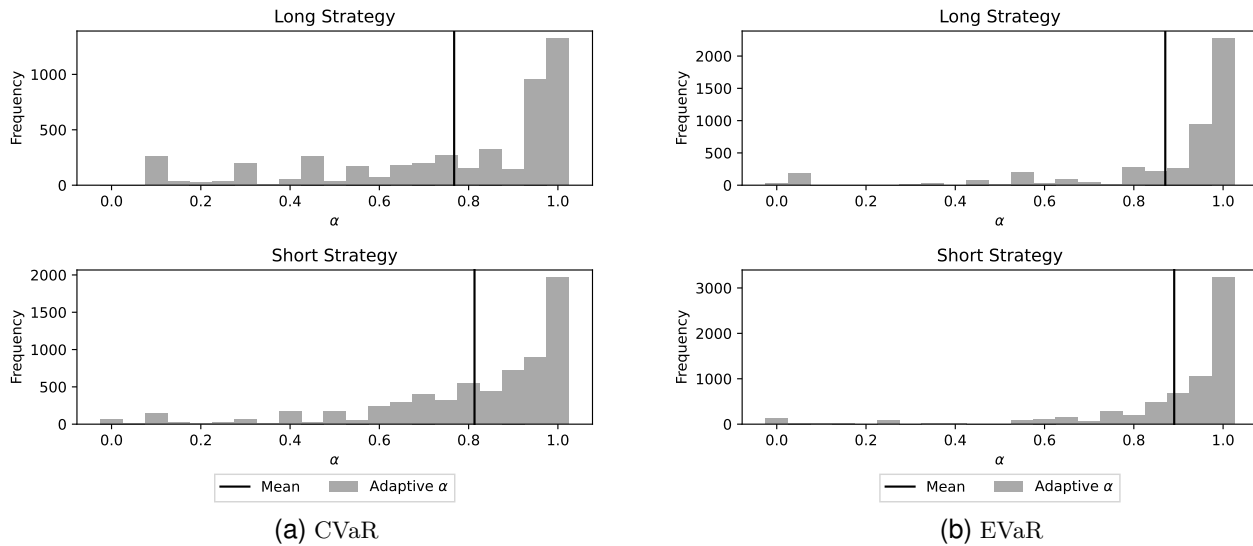


Fig. 9. The optimized values of α that the adaptive trading strategy chooses on the test set. Most of the time a high value of α is chosen, meaning that the trading strategy has a strong confidence in the model. In uncertain scenarios, α is reduced to avoid consistent losses.

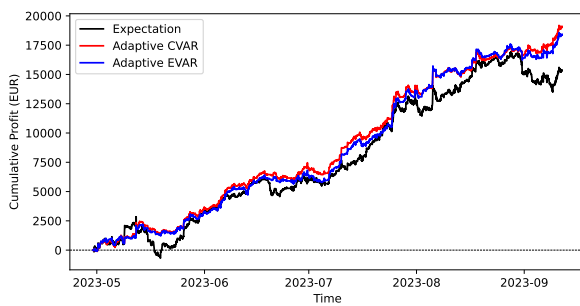


Fig. 10. The accumulated profits of the adaptive trading strategies. Although they are relatively similar to the expectation strategy, the adaptive strategies only requires a fraction of the trades.

no. 5, pp. 559 – 570, 2000.

Robin Bruneel Robin Bruneel obtained a Bachelor's degree (BSc) in Electrical Engineering and a Master's in Mathematical Engineering from KU Leuven, Belgium in 2020 and 2022, respectively. Currently, he is a data scientist at Amplifino and pursues a PhD at the Department of Electrical Engineering (ESAT) of KU Leuven. His research interests are risk-averse trading strategies and probabilistic forecasting models in the energy sector.

Mathijs Schuurmans Obtained a MSc in Mathematical Engineering and a PhD in Control and Optimization from KU Leuven in 2018 and 2023, respectively. He is currently a postdoc at the Department of Electrical Engineering (ESAT) at the same university. His research is focused on learning-based estimation and control of stochastic systems, focusing on distributionally robust approaches for safety-critical applications.

Panagiotis Patrinos Panagiotis (Panos) Patrinos is associate professor at the Department of Electrical Engineering (ESAT) of KU Leuven, Belgium. In 2014 he was a visiting professor at Stanford University. He received his PhD in Control and Optimization, M.S. in Applied Mathematics and M.Eng. in Chemical Engineering from the National Technical University of Athens in 2010, 2005 and 2003, respectively. After his PhD he held postdoc positions at the University of Trento and IMT Lucca, Italy, where he became an assistant professor in 2012. His current research interests lie in the intersection of optimization, control and learning. In particular he is interested in the theory and algorithms for structured nonconvex optimization as well as learning-based, model predictive control with a wide range of applications including autonomous vehicles, machine learning and signal processing. He is the co-recipient of the 2020 best paper award in International Journal of Circuit Theory & Applications

- [16] G. McLachlan and D. Peel, *Finite mixture models.*, ser. Wiley series in probability and statistics. Applied probability and statistics section. New York: Wiley, 2000.
- [17] A. Niculescu-Mizil and R. Caruana, "Predicting good probabilities with supervised learning," 01 2005, pp. 625–632.
- [18] A. Cucchiara, "Applied logistic regression," *Technometrics*, vol. 34, no. 3, pp. 358–359, 1992.
- [19] D. Böhning, "Multinomial logistic regression algorithm," *Annals of the Institute of Statistical Mathematics*, vol. 44, no. 1, pp. 197–200, Mar 1992.
- [20] R. Koenker and K. F. Hallock, "Quantile regression," *Journal of Economic Perspectives*, vol. 15, no. 4, pp. 143–156, December 2001.
- [21] R. T. Rockafellar, S. Uryasev *et al.*, "Optimization of conditional value-at-risk," *Journal of risk*, vol. 2, pp. 21–42, 2000.
- [22] A. Ahmadi-Javid, "Entropic value-at-risk: A new coherent risk measure," *Journal of Optimization Theory and Applications*, vol. 155, no. 3, pp. 1105–1123, Dec 2012.
- [23] M. Schuurmans, A. Katriniok, C. Meissen, H. E. Tseng, and P. Patrinos, "Safe, learning-based mpc for highway driving under lane-change uncertainty: A distributionally robust approach," *Artificial Intelligence*, vol. 320, p. 103920, 2023.
- [24] N. Meinshausen, "Quantile regression forests," *Journal of Machine Learning Research*, vol. 7, no. 35, pp. 983–999, 2006.
- [25] T. Gneiting and M. Katzfuss, "Probabilistic forecasting," *Annual Review of Statistics and Its Application*, vol. 1, no. 1, pp. 125–151, 2014.
- [26] H. Hersbach, "Decomposition of the continuous ranked probability score for ensemble prediction systems," *Weather and Forecasting*, vol. 15,